UDC 629.7.05:623.46:519.68:531.391
Original scientific paper
Received: 14.11.2003.

Algorithm of direct gyroscope stabilizer control and correction

Zbigniew Koruba
Kielce University of Technology, Faculty of Mechatronics and Machine Building,
Chair of Vehicles and Mechanical Equipment, Al. Tysiaclecia PP 3, 25-314 Kielce, POLAND
e-mail: ksmzko@tu.kielce.pl

SUMMARY

The paper presents the analysis of stabilisation and accuracy of gyroscope stabilizer, which is used for automatic control and homing of aerial objects. The existence of through relations between channels of multiaxial gyroscope stabilizer causes errors in the operation of those devices. Therefore, it is necessary to select the optimum parameters for all elements of stabilization channels. The algorithm of the optimum selection of the above-mentioned parameters and the results of computer simulation investigations are given.

***Key words**: Gyroscope stabilizer, homing of aerial objects, automatic control, stabilization element, Golubiencev optimization method.*

1. INTRODUCTION

Modern gyroscope stabilizers (GS) are highly complicated electromechanical devices equipped with microprocessors and blocks exchanging information with the board computer [1, 2, 3]. They are geared, first of all, to: a) stabilize platform angular position with reference to one, two or three axes; b) measure inclination, deflection and tilt angles; c) set the program-run motion of an aerial object; d) generate control moments for other measurement elements of stabilization (e.g. target co-ordinator in a homing missile gyroscope compass aboard, etc.) or to change the motion of an aerial object [4, 5, 6] (e.g. a spaceship or small calibre homing missile).

The paper discusses an active three-degree direct gyroscope stabilizer (DGS), which might be applied to the homing of light aerial objects (AOs), such as, e.g., homing bombs. DGS is designed to generate control moments in the tilt, inclination and deflection channel in accordance with the assumed homing algorithm.

Apart from homing, positioning and programme-run manoeuvring, AO stabilizing is also performed.

The operation principle of each control channel - both at the basic operational mode and at the initial setting - is analogous with the operation principle of a single-axed gyroscope stabilizer. The only significant difference results from the occurrence of through relations between the channels.

Through relations between the channels of GS force stabilization lead to errors made by these devices. The physical realization of those relations consists in the fact that when the platform is deflected with reference to, e.g., inclination axis, the deflection channel gyroscope as an inert body, connected with the base by friction forces, will also react to deflection. It should be mentioned, however, that when the interference along the deflection line is absent, the above-mentioned reaction will not take place. The conclusion is that the device analysis cannot be limited to the investigations concerning two independent single-axed GSs, i.e. to the solutions to two differential equations of the second order (whose structure is very close to equations describing the motion of an astatic gyroscope of three degrees of freedom) but it must be the system of four such equations. Obviously, it is not possible to obtain an analytical solution to a characteristic equation of 8^{th} degree - so it must be carried out with a numerical method.

Thus through relations account for considerable complications of GS stability and accuracy investigations. Moreover, an optimum selection of parameters of individual elements of control channels should be made, which was conducted with modified Golubiencev optimization method. Due to this method, it was possible to unambiguously determine the values of coefficients of amplifications and damping for one- and two-axed gyroscope stabilizer. Those are selected in such a manner so that transition processes can disappear over the shortest possible time. DGS is a strongly non-linear system, so at high values of its angular deflections and angular velocities, there arise errors in the motion actually performed with reference to the pre-set one. DGS programme-run control in the non-linear range of operation and under the conditions of interference impact must be accompanied by additional optimum control in the closed system. The algorithm for the selection of the optimum parameters of DGS control presented in the paper contributes to the minimization of discrepancies between the pre-set and performed path. It is carried out due to the possibility of changing, in real time, the regulator coefficients, depending on changes in angular velocity of self rotations in the function of time. If we deal with gyroscopes or regulators of already known parameters, the optimum angular velocity of self rotation can be selected, being the function of those parameters.

The paper will discuss the possibility of applying a direct gyroscope stabilizer (DGS) to the control and stabilization of aerial objects. DGSs, also called gyroscope executive organs (GEO), are designed to generate control moments (gyroscope rudders) and damping moments (gyroscope dampers) in the control systems of aerial objects.

At first, DGSs were used to reduce ships swaying or to stabilize single-rail cars and two-wheeled vehicles. Later they also served as the stabilization of ship guns.

The 1950s, the beginning of the space exploration era, stirred up wide interest in DGSs. It turned out that, in comparison with other executive organs, DGSs demonstrated unmatched accuracy, moreover, they were energy saving.

Depending on the operating range, the systems with DGSs are divided into semi-passive and active.

The main task of semi-passive systems is to damp vibrations of an aerial object (AO). The expenditure of energy in GEOs results mainly from the necessity of maintaining constant values of gyroscopes angular momenta. Active range systems account for AOs stabilization, orientation and program-run manoeuvres.

GEOs are constructed on the basis of two- and three-degree gyroscopes. Most frequently, in both types of GEOs doubled gyroscopes are used. Moreover, gyroscopes used in GEOs are those with the classical Cardan suspension, doubled gyroscopes with conical suspension and non-Cardan suspension (spherical) gyroscopes.

2. MODEL OF THE MOTION OF AERIAL OBJECT (AO) - GYROSCOPE SYSTEM

Let us consider an aerial object with a gyroscope located on it or inside it (Figure 1). Assume first, that the gyroscope symmetrical rotor can revolve around axis AA, which coincides with AO longitudinal axis. As the rotor is symmetrical in respect of fast rotation axis, the distribution of masses of the whole system of AO-gyroscope does not change while the rotor rotates. Therefore, the system moments of inertia will be constant and the system motion can be described with the same method as the motion of a single rigid body.

Thus, AO is assumed to be a non-deformable (rigid) body of constant mass. Hence the motion of AO-gyroscope system can be stated with two systems of equations, which describe the motion of the system centre of mass and the motion around the centre of mass. In addition, the case considered will be the simplest one, when the rotor axis O_{x_3} is, at the same time, the principal central axis of inertia of AO (axis O_x).

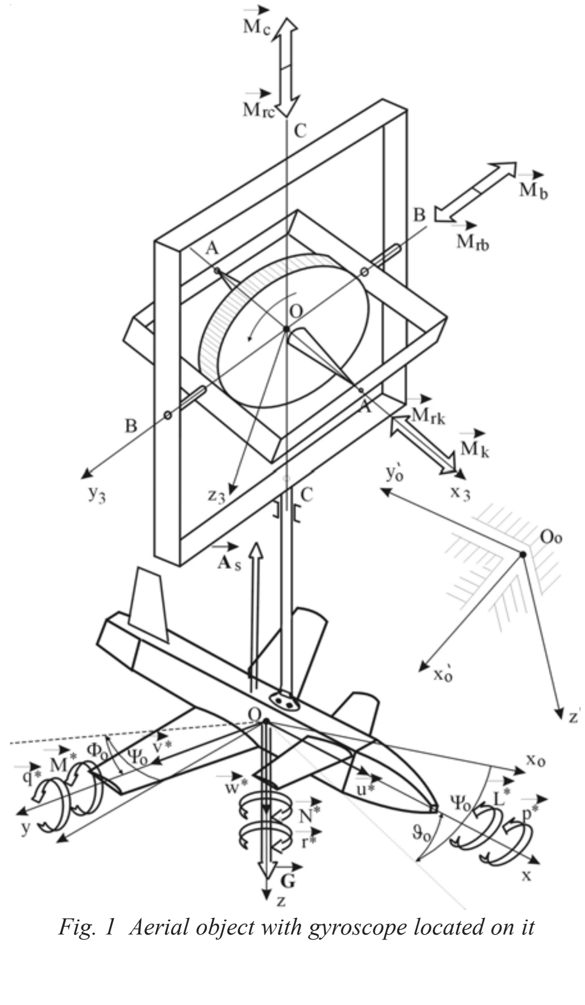

Fig. 1 Aerial object with gyroscope located on it

The equation of AO translatory motion in the connected co-ordinate system O_{xyz} reads as follows:

$$m_o\left(\frac{d\boldsymbol{u}^*}{dt}+\boldsymbol{w}^*\boldsymbol{q}^*-\boldsymbol{v}^*\boldsymbol{r}^*\right)=\boldsymbol{F}_x \tag{1a}$$

$$m_o\left(\frac{d\boldsymbol{v}^*}{dt}+\boldsymbol{u}^*\boldsymbol{r}^*-\boldsymbol{w}^*\boldsymbol{p}^*\right)=\boldsymbol{F}_y \tag{1b}$$

$$m_o\left(\frac{d\boldsymbol{w}^*}{dt}+\boldsymbol{p}^*\boldsymbol{v}^*-\boldsymbol{q}^*\boldsymbol{u}^*\right)=\boldsymbol{F}_z \tag{1c}$$

where m_0 is mass of AO-gyroscope system; $\boldsymbol{u}^*$, $\boldsymbol{v}^*$ and $\boldsymbol{w}^*$ are components of AO linear velocity in the related co-ordinate system O_{xyz}; $\boldsymbol{p}^*$, $\boldsymbol{q}^*$ and $\boldsymbol{r}^*$ are components of AO angular velocity in the related co-ordinate system O_{xyz} and $\boldsymbol{F}_x$, $\boldsymbol{F}_y$ and $\boldsymbol{F}_z$ are components of the principal vector of external forces acting on AO, at the same time:

$$\begin{bmatrix}\boldsymbol{F}_x\\ \boldsymbol{F}_y\\ \boldsymbol{F}_z\end{bmatrix}=\begin{bmatrix}\boldsymbol{A}_x^s+\boldsymbol{G}_x\\ \boldsymbol{A}_y^s+\boldsymbol{G}_y\\ \boldsymbol{A}_z^s+\boldsymbol{G}_z\end{bmatrix} \tag{2}$$

In exactly the same co-ordinate system, however, the equation of the motion of a spherical AO reads as follows:

$$J_{ox}\frac{d\boldsymbol{p}_s}{dt}+\left(J_{oz}-J_{oy}\right)\boldsymbol{q}^*\boldsymbol{r}^*=\boldsymbol{L}^* \tag{3a}$$

$$J_{oy}\frac{d\boldsymbol{q}^*}{dt}+\left(J_{ox}-J_{oz}\right)\boldsymbol{p}^*\boldsymbol{r}^*=\boldsymbol{M}^* \tag{3b}$$

$$J_{oz}\frac{d\boldsymbol{r}^*}{dt}+\left(J_{oy}-J_{ox}\right)\boldsymbol{p}^*\boldsymbol{q}^*=\boldsymbol{N}^* \tag{3c}$$

where: J_{ox}, J_{oy} and J_{oz} are principal central moments of AO inertia in relation to the individual axes of the system O_{xyz}; $\boldsymbol{L}^*$, $\boldsymbol{M}^*$ and $\boldsymbol{N}^*$ are components of the vector of the principal moment of external forces, at the same time:

$$\begin{bmatrix}\boldsymbol{L}^*\\ \boldsymbol{M}^*\\ \boldsymbol{N}^*\end{bmatrix}=\begin{bmatrix}\boldsymbol{L}_A+\boldsymbol{L}_G\\ \boldsymbol{M}_A+\boldsymbol{M}_G+M_b^s\\ \boldsymbol{N}_A+\boldsymbol{N}_G+M_c^s\end{bmatrix}$$

where: $\boldsymbol{L}_A$, $\boldsymbol{M}_A$ and $\boldsymbol{N}_A$ are components of the vector of the principal moment of aerodynamic forces; $\boldsymbol{L}_G$, $\boldsymbol{M}_G$ and $\boldsymbol{N}_G$ are components of the vector of the principal moment of gravity forces; M_b^s and M_c^s are moments of forces controlling the aerial object.

<u>*Kinematic relations between angular velocities*</u>

$$\frac{d\Psi_o}{dt}=\left(\boldsymbol{q}^*\sin\Phi_o+\boldsymbol{r}^*\cos\Phi_o\right)\sec\Theta_o \tag{4a}$$

$$\frac{d\Theta_o}{dt}=\boldsymbol{q}^*\cos\Phi_o-\boldsymbol{r}^*\sin\Phi_o \tag{4b}$$

$$\frac{d\Phi_o}{dt}=\boldsymbol{p}^*+\left(\boldsymbol{q}^*\sin\Phi_o+\boldsymbol{r}^*\cos\Phi_o\right)tg\Theta_o \tag{4c}$$

where Ψ_o, Θ_o and Φ_o are angles of AO longitudinal axis deflection, inclination and tilt.

<u>*Kinematic relations between linear velocities (AO flight path)*</u>

$$\frac{dx_o}{dt}=\boldsymbol{u}^*\cos\Theta_o\cos\Psi_o+\boldsymbol{v}^*\left(\sin\Phi_s\sin\Theta_o\cos\Psi_o-\cos\Phi_o\sin\Psi_o\right)+\boldsymbol{w}^*\left(\cos\Phi_o\sin\Theta_o\cos\Psi_o+\sin\Phi_o\sin\Psi_o\right) \tag{5a}$$

$$\frac{dy_o}{dt}=\boldsymbol{u}^*\cos\Theta_o\sin\Psi_o+\boldsymbol{v}^*\left(\sin\Phi_o\sin\Theta_o\sin\Psi_o+\cos\Phi_o\cos\Psi_o\right)+\boldsymbol{w}^*\left(\cos\Phi_o\sin\Theta_o\cos\Psi_o+\sin\Phi_o\sin\Psi_o\right) \tag{5b}$$

$$\frac{dz_o}{dt}=-\boldsymbol{u}^*\sin\Theta_o+\boldsymbol{v}^*\sin\Phi_s\cos\Theta_o+\boldsymbol{w}^*\cos\Phi_o\cos\Theta_o \tag{5c}$$

3. THE CONTROL OF THE AO-GYROSCOPE SYSTEM

In the case under consideration, the control of the aerial object consists in forced changes in the gyroscope axis position in relation to AO body (Figure 2). That task is carried out by control moments M_b^s and M_c^s, which make the AO body axis turn in relation to the inertial reference system $Ox_oy_oz_o$ (in relation to the Earth). Therefore, the gyroscope considered will be called a control moment gyro.

The equations of the gyroscope motion for such a case, when the inertia of frames is disregarded, will be as follows:

$$J_{gk}\frac{d\omega_{gy_3}}{dt}-J_{gk}\omega_{gx_2}\omega_{gz_3}+J_{go}n_g\omega_{gz_3}=M_b^s-M_{rb} \tag{6a}$$

$$J_{gk}\frac{d}{dt}\left(\omega_{gz_3}\cos\vartheta_g\right)-J_{go}n_g\frac{d\vartheta_g}{dt}\cos\vartheta_g+J_{gk}\omega_{gx_1}\omega_{gy_3}-J_{go}\omega_{gz_3}\omega_{gy_1}\cos\vartheta_g=M_c^s-M_{rc} \tag{6b}$$

where: $\omega_{gx_1}=p^*\cos\psi_g+q^*\sin\psi_g$; $\omega_{gy_1}=-p^*\sin\psi_g+q^*\cos\psi_g$; $\omega_{gz_1}=\dot{\psi}_g+r^*$

$$\omega_{gx_2} = \left(p^* \cos\psi_g + q^* \sin\psi_g\right)\cos\vartheta_g - \left(r^* + \dot{\psi}_g\right)\sin\vartheta_g$$
$$\omega_{gy_2} = -p^* \sin\psi_g + q^* \cos\psi_g + \dot{\vartheta}_g$$
$$\omega_{gz_2} = \left(p^* \cos\psi_g + q^* \sin\psi_g\right)\sin\vartheta_g + \left(r^* + \dot{\psi}_g\right)\cos\vartheta_g$$

$$\omega_{gx_3} = \left(p^* \cos\psi_g + q^* \sin\psi_g\right)\cos\vartheta_g - \left(r^* + \dot{\psi}_g\right)\sin\vartheta_g + \dot{\Phi}_g$$
$$\omega_{gy_3} = -p^* \sin\psi_g + q^* \cos\psi_g + \dot{\vartheta}_g$$
$$\omega_{gz_3} = \left(p^* \cos\psi_g + q^* \sin\psi_g\right)\sin\vartheta_g + \left(r^* + \dot{\psi}_g\right)\cos\vartheta_g$$

where: J_{go} and J_{gk} are longitudinal and transverse moments of inertia of gyroscope rotor, respectively; ϑ_g and ψ_g are angles stating the gyroscope axis position in space; Φ_g is angle of rotation of gyroscope rotor; M_{rb} and M_{rc} are moments of friction force in the bearings of internal and external frame, respectively.

Linearized equations of gyroscope motion will take on the following form:

$$J_{gk}\frac{d}{dt}\left(\dot{\vartheta}_g + q^*\right) + J_{go}\underbrace{\left(\dot{\Phi}_g + p^*\right)}_{n_g}\left(\dot{\psi}_g + r^*\right) = M_b^s - M_{rb} \quad (7a)$$

$$J_{gk}\frac{d}{dt}\left(\dot{\psi}_g + r^*\right) - J_{go}\underbrace{\left(\dot{\Phi}_g + p^*\right)}_{n_g}\left(\dot{\vartheta}_g + q^*\right) = M_c^s - M_{rc} \quad (7b)$$

The diagram of the control of the AO-gyroscope system is presented in Figure 3.

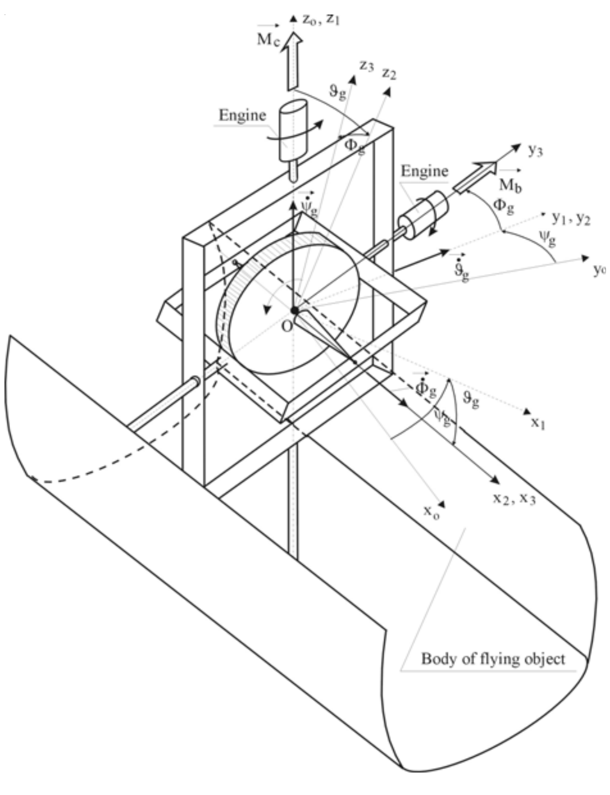

Fig. 2 Gyroscope with rotor axis capable of changing position in respect of aerial object

Control moments $\boldsymbol{M}_b^s$ and $\boldsymbol{M}_c^s$, which appear in the right-hand sides of Eqs. (6) and (7), will be given the form:

$$\begin{aligned}\boldsymbol{M}_b^s &= \boldsymbol{M}_b^p + \boldsymbol{M}_b^k \\ \boldsymbol{M}_c^s &= \boldsymbol{M}_c^p + \boldsymbol{M}_c^k\end{aligned} \quad (8)$$

Quantities $\boldsymbol{M}_b^p$ and $\boldsymbol{M}_c^p$, in Eq. (8), are program-run control moments, determined from the dynamics inverse problem. If friction in gyroscope bearings is assumed to be viscous and a temporary assumption is made that AO moves along a rectilinear path, the moments determined from Eq. (7) will take on the form:

$$M_b^p = J_{gk}\frac{d}{dt}\left(\dot{\vartheta}_{gz} + q^*\right) + J_{go}n_g\left(\dot{\psi}_{gz} + r^*\right) + \eta_b\vartheta_{gz} \quad (9a)$$

$$M_c^p = J_{gk}\frac{d}{dt}\left(\dot{\psi}_{gz} + r^*\right) - J_{go}n_g\left(\dot{\vartheta}_{gz} + q^*\right) + \eta_c\psi_{gz} \quad (9b)$$

where ϑ_{gz} and ψ_{gz} are desirable angles of gyroscope axis position.

Controls $\boldsymbol{M}_b^p$ and $\boldsymbol{M}_c^p$ should be selected in such a manner so that the aerial object would move along a desired path or adopt a pre-set position in space.

Quantities $\boldsymbol{M}_b^k$ and $\boldsymbol{M}_c^k$, on the other hand, are correction controls determined by means of complex optimization, with the use of the LQR method and the modified Golubiencew optimization method, the algorithm of which is presented in Figure 4. Correction controls become a necessity when interference occurs and non-linearity affects AO-gyroscope system. Those controls are worked out in the regulator on the basis of discrepancy parameters, i.e. deviation of the actual motion of the aerial vehicle from the pre-set motion.

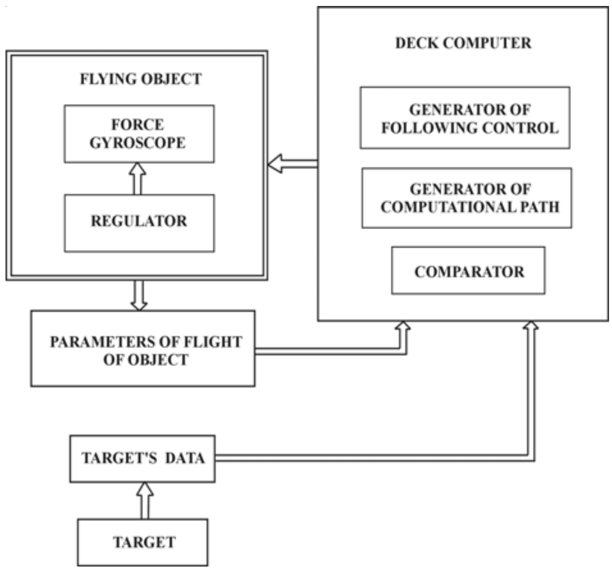

Fig. 3 Functional diagram of control of AO-gyroscope system

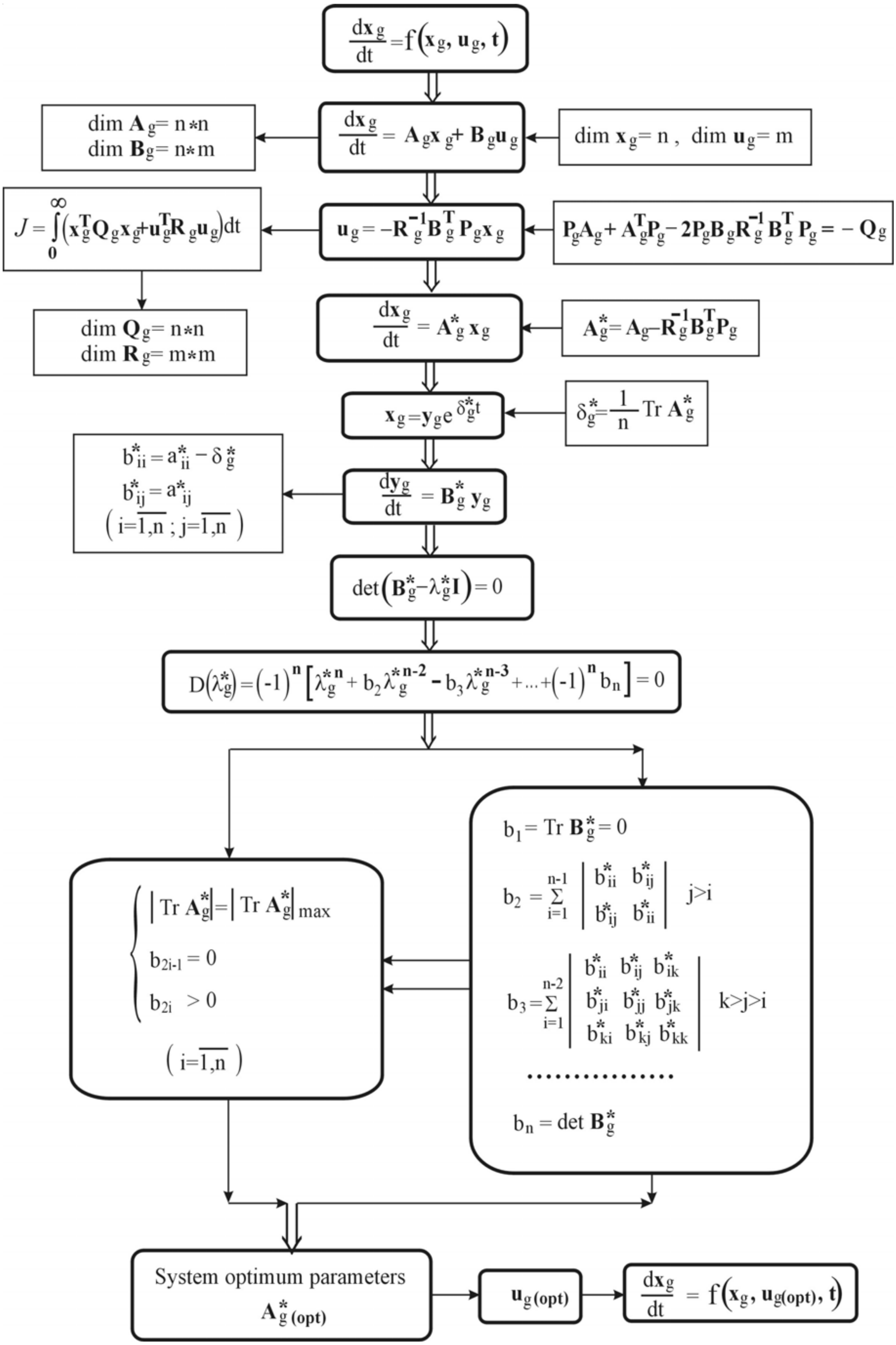

Fig. 4 Diagram of optimization with modified Golubiencew method

4. OPTIMISATION OF CONTROL MOMENT GYRO

The impact of the effect of the base: $p^*=q^*=r^*=0$, friction in bearings: $M_{rb}=M_{rc}=0$ and program-run control: $M_b{}^p=M_c{}^p=0$ will be disregarded in Eqs. (9) in order to select the optimum correction control. Then, with the use of states space method, we obtain simplified Eqs. (9) in the vector-matrix form:

$$\frac{d\boldsymbol{x}_g}{d\tau} = \boldsymbol{A}_g \cdot \boldsymbol{x}_g + \boldsymbol{B}_g \cdot \boldsymbol{u}_g \qquad (10)$$

where:

$$\boldsymbol{x}_g = \begin{bmatrix} \vartheta_g & \frac{d\vartheta_g}{d\tau} & \psi_g & \frac{d\psi_g}{d\tau} \end{bmatrix}^T, \quad \boldsymbol{u}_g = \begin{bmatrix} M_b^k & M_c^k \end{bmatrix}^T,$$

$$\tau = \Omega \cdot t, \quad \Omega = \frac{J_{go} n_g}{J_{gk}},$$

$$\boldsymbol{A}_g = \begin{bmatrix} 0 & 1 & 0 & 0 \\ 0 & 0 & 0 & -1 \\ 0 & 0 & 0 & 1 \\ 0 & 1 & 0 & 0 \end{bmatrix}, \quad \boldsymbol{B}_g = \begin{bmatrix} 0 & 0 \\ c_b & 0 \\ 0 & 0 \\ 0 & c_c \end{bmatrix},$$

$$c_b = c_c = \frac{1}{J_{gk}\Omega^2}$$

The law of control will be presented in the following form:

$$\boldsymbol{u}_g = -\boldsymbol{K}_g \cdot \boldsymbol{x}_g \qquad (11)$$

The conjugation matrix $\boldsymbol{K}_g$, which occurs in Eq. (3), is determined from the following dependence:

$$\boldsymbol{K}_g = \boldsymbol{R}_g^{-1} \boldsymbol{B}_g^T \boldsymbol{P}_g \qquad (12)$$

Matrix $\boldsymbol{P}_g$ is a solution to Riccati algebraic equation:

$$\boldsymbol{A}_g^T \boldsymbol{P}_g + \boldsymbol{P}_g \boldsymbol{A}_g - 2\boldsymbol{P}_g \boldsymbol{B}_g \boldsymbol{R}_g^{-1} \boldsymbol{B}_g^T \boldsymbol{P}_g + \boldsymbol{Q}_g = \boldsymbol{0} \qquad (13)$$

Weight matrices $\boldsymbol{R}_g$ and $\boldsymbol{Q}_g$, which occur in Eqs. (12) and (13), reduced to diagonal form, are selected experimentally; they are sought starting with equal values:

$$q_{ii} = \frac{1}{2x_{i_{max}}}, \quad r_{ii} = \frac{1}{2u_{i_{max}}}, \quad (i = 1,2,..8) \qquad (14)$$

where x_{imax} is the maximum range of changes in the i^{th} state variable value; u_{imax} is the maximum range of changes in the i^{th} control variable value.

On obtaining numerical solution to Riccati matrix equation, Eq. (13), and determining amplifications matrix $\boldsymbol{K}_g$, it could be noted that for the case under consideration, the matrix individual components fulfil the following dependence:

$$\begin{aligned} &k_{11} = k_{23} = \bar{k}_b, \\ &k_{12} = k_{14} = k_{22} = k_{24} = \bar{h}_g, \\ &k_{21} = -k_{13} = \bar{k}_c \end{aligned} \qquad (15)$$

After amplifications coefficients from Eq. (15) are inserted into Eq. (11), the correction controls will take the following form:

$$u_b = -\bar{k}_b \vartheta_g + \bar{k}_c \psi_g - \bar{h}_g \frac{d\vartheta_g}{d\tau} \qquad (16a)$$

$$u_c = -\bar{k}_c \vartheta_g - \bar{k}_b \psi_g - \bar{h}_g \frac{d\psi_g}{d\tau} \qquad (16b)$$

where:

$$\bar{k}_b = \frac{k_b}{J_{gk}\Omega^2}, \quad \bar{k}_c = \frac{k_c}{J_{gk}\Omega^2}, \quad \bar{h}_g = \frac{h_g}{J_{gk}\Omega} \qquad (17)$$

Thus when Eq. (16) is taken into account, the gyroscope system in the closed system, Eq. (10), will be equivalent to a new form:

$$\frac{d\boldsymbol{x}_g}{d\tau} = \boldsymbol{A}_g^* \cdot \boldsymbol{x}_g \qquad (18)$$

where:

$$\boldsymbol{A}_g^* = \begin{bmatrix} 0 & 1 & 0 & 0 \\ -\bar{k}_b & -\bar{h}_g - b_b & +\bar{k}_c & 1 \\ 0 & 0 & 0 & 1 \\ -\bar{k}_c & -1 & -\bar{k}_b & -\bar{h}_g - b_c \end{bmatrix} \qquad (19)$$

From now on, the friction in gyroscope suspension bearings will be regarded as negligibly small, i.e. $b_b=b_c=0$. For the gyroscope system described in such a manner, we will be additionally seeking such parameters and relations between them so that the transition process damping would be the shortest. In order to achieve that, the modified Golubiencew optimization method [7] will be employed (Figure 4).

On the basis of Hurwitz stability conditions as well as the modified Golubiencew optimization method [4], we will obtain the following system of equations and inequalities:

$$\bar{k}_b > 0, \ \bar{k}_c > 0, \ \bar{h}_g > 0 \qquad (20a)$$

$$2\bar{k}_b - \frac{1}{2}\bar{h}_g^2 + 1 > 0 \qquad (20b)$$

$$\bar{k}_c = \frac{1}{2}\bar{h}_g \qquad (20c)$$

$$\frac{1}{16}\bar{h}_g^4 + \frac{1}{4}\bar{h}_g^2 - \frac{1}{2}\bar{h}_g^2\bar{k}_b - \bar{h}_g\bar{k}_c + \bar{k}_b^2 + \bar{k}_c^2 > 0 \qquad (20d)$$

If we consider the condition of maximization of the absolute value of matrix trace $\boldsymbol{A}_g^*$:

$$\left| Tr\boldsymbol{A}_g^* \right| \to max \qquad (21)$$

from inequality Eq. (20b), we will obtain the following value for a damping coefficient:

$$\bar{h}_g = \sqrt{2 + 4\bar{k}_b} \qquad (22)$$

Inserting Eq. (22) into Eq. (20c), we will receive:

$$\bar{k}_c = \frac{1}{2}\sqrt{2 + 4\bar{k}_b} \qquad (23)$$

Taking into account Eqs. (17), we have:

$$h_g = \sqrt{2J_{go}^2 n_g^2 + 4J_{gk}k_b} \qquad (24)$$

$$k_c = \frac{1}{2}\sqrt{2J_{go}^2 n_g^2 + 4J_{gk}k_b} \cdot \frac{J_{go}^2 n_g^2}{J_{gk}} \qquad (25)$$

In this way, coefficients $\bar{h}_g$ and $\bar{k}_c$ are unambiguously specified as functions of gyroscope parameters J_{go}, J_{gk} and n_g as well as coefficient $\bar{k}_b$. The latter should satisfy stability conditions and technical limitations resulting from the gyroscope construction itself.

The dependence derived above can be applied to gyroscope control under the conditions of changeable angular velocity of self-rotation (e.g. in some homing bombs or in systems for target search with a wide range of gyroscope axis angular deflections). Then it is necessary to continually take measurements of value $n_g(t)$ and update, in real time, the values of regulator coefficients h_g and k_c in accordance with dependence Eqs. (24) and (25). The coefficient k_b is pre-set in a programme-run fashion. That allows adaptive gyroscope control. If many other gyroscope parameters are changeable in time, the algorithm for adaptive gyroscope control should be applied [8].

Figure 5 shows the results of the control of gyroscope axis in moving target tracking, where the optimum regulator is applied. Its coefficients are determined from Eqs. (24) and (25).

In the actual motion of the gyroscope, we deal with kinematic effect of AO deck, which takes the form of angular velocities ***p****, ***q**** and ***r****. In turn, the kinematic effect of the deck manifests due to friction in suspension bearings. Program-run controls are, therefore executed with a certain error and the actual AO flight path does not coincide with the computed one. Thus, the eventual correction controls for the AO-gyroscope system should take the form:

$$M_b^k = -\bar{k}_b\left(\vartheta_g - \vartheta_{gz}\right) + \bar{k}_c\left(\psi_g - \psi_{gz}\right) - \bar{h}_g\left(\frac{d\vartheta_g}{d\tau} - \frac{d\vartheta_{gz}}{d\tau}\right) \qquad (26)$$

$$M_b^k = -\bar{k}_b\left(\vartheta_g - \vartheta_{gz}\right) + \bar{k}_c\left(\psi_g - \psi_{gz}\right) - \bar{h}_g\left(\frac{d\vartheta_g}{d\tau} - \frac{d\vartheta_{gz}}{d\tau}\right) \qquad (27)$$

If gyroscope is suspended on Cardan joint and given three degrees of freedom, it gets isolated from the aerial object deck. Then, the equations of AO motion and gyroscope motion are no longer coupled. Further in the paper, we will consider examples of one- and two-axial gyroscope stabilizers, which are independent of AO motions. They are most frequently applied to the inertial systems of navigation of aerial objects.

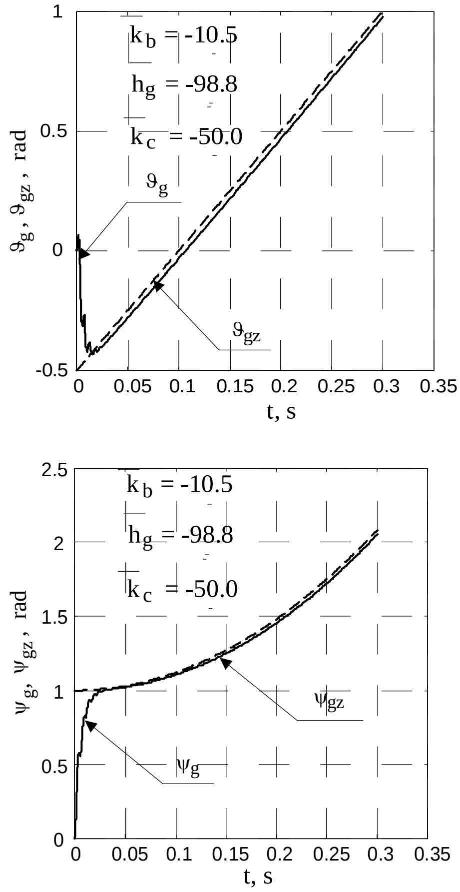

Fig. 5 Results of gyroscope axis control with the optimum regulator application to motionless point tracking: change in angular deflections as the function of time

5. OPTIMUM CORRECTION FOR ONE-AXIAL DIRECT GYROSCOPE STABILIZER (OADGS)

We will discuss a gyroscope of three degrees of freedom, borne on the base *P* (aerial object deck) (Figure 6).

If we impart rotation around the suspension external axis CC to the gyroscope base, due to friction forces unavoidably occurring in resistance *a* and *b*, the moment M_c will affect the gyroscope, trying to turn it in respect of axis CC. The moment of friction forces will tend to make the gyroscope follow the moving base. Yet, as we know, the gyroscope primary motion will be made not in the direction the moment M_c acts, but around the suspension external axis BB, which is perpendicular to vector $\vec{M}_c$ direction. The angular velocity of the discussed precession motion will be expressed:

$$\dot{\vartheta}_g = \frac{M_c}{J_{go} n_g \cos \vartheta_g} \tag{28}$$

While the gyroscope moves around axis BB with velocity $\dot{\vartheta}_g$, a gyroscope moment appears in its system:

$$M_g = J_{go} n_g \dot{\vartheta}_g \tag{29}$$

and it acts around axis $0y_3$ related to the gyroscope.

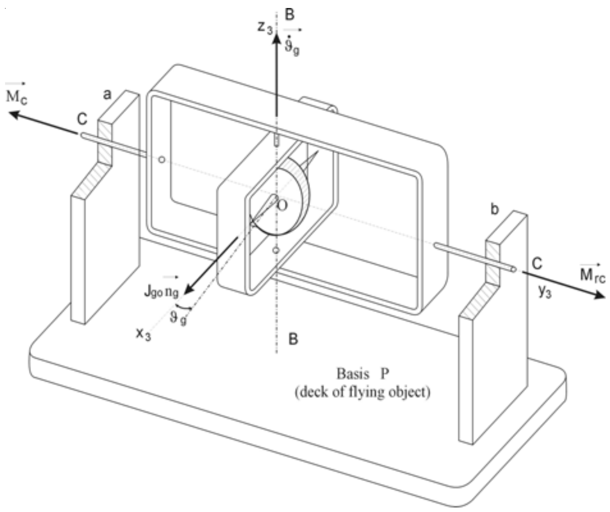

Fig. 6 Diagram of one-axial gyroscope stabilizer

In the general case, gyroscope moment M_g projection onto the external suspension axis CC will equal:

$$M_{gc} = M_g \cos \vartheta_g = J_{go} n_g \frac{M_c}{J_{go} n_g \cos \vartheta_g} \cos \vartheta_g = M_c \tag{30}$$

and it will have the sense opposite to the external moment M_c.

As we can see, the component of the gyroscope moment $M_g \cos \vartheta_g$ counterbalances the external moment M_c, acting on the gyroscope, thus maintaining the stability of the position of the gyroscope external frame in respect of the gyroscope suspension axis *CC*.

One-axial gyroscope stabilizer is one of the simplest types (Figure 7). Its structural diagram is analogous with that of astatic gyroscope of three degrees of freedom suspended on Cardan joint (Figure 6). The only difference is the platform, stabilized in respect of a selected axis, fixed to the external frame. Thus the principle of operation of one-axial stabilizer does not differ from that of a gyroscope of three degrees of freedom. It will be enough to introduce the angle of deflection ψ_p of the platform instead of the angle of deflection ψ_g of the external frame and also account for the damper μ_g between the gyroscope frame and the platform. The main task of one-axis stabilizer is to make the platform (where measurement devices might be located) position, in respect of a selected axis in space, independent of the base (AO deck) angular motions. Because of the large mass of the external frame in comparison with the internal one, however, the bearing of the axis of the external frame (called stabilization axis) carries high loads. Those yield large friction moment, which in turn, leads to the internal frame precession. At small gyroscope moment of momentum, the gyroscope moment appearing in response to friction moment along the stabilization axis, might result, over a short time interval, in the folding of the frames (the angle between them equals zero), which means the device loses its basic property. In order to prevent this unfavourable incident happen, the stabilizer system is equipped with a stabilizing electric engine with a converting amplifier (Figure 6). Then, after the interference moment appears, the gyroscope internal frame will deflect by angle ϑ_g, the value of which will be measured with the precession angle sensor and transmitted to the amplifier as an electric signal. Later, the amplified and converted signal is passed to the stabilizing engine, which will apply moment M_s, of the sense opposite to that of the interference moment M_{zc}, to the stabilization axis. As the process develops, both moments become equal $M_s = M_{zc}$, the gyroscope precession is ceased and the platform keeps, with the pre-set accuracy, its invariable position in the inertial space in relation to the stabilization axis [2, 3].

In this way, simultaneous operation of the gyroscope of two degrees of freedom and the stabilizing engine ensures force based gyroscope stabilization. However, due to friction in the bearings of gyroscope and platform suspensions, the external interference in the form of kinematic input (e.g., AO deck vibrations, AO linear and angular accelerations or the Earth rotational motion), affecting the stabilizer base leads to errors in stabilizer position. In order to minimize the above-mentioned parameters, it is necessary to select the optimum parameters of gyroscope stabilizer (characteristics of stabilising engine, damper and gyroscope moment of momentum).

Taking into account the above-mentioned formal similarity between OADGS and a gyroscope of three degrees of freedom, we will rely on motion equations of the latter writing them as follows:

$$J_p \frac{d^2 \psi_p}{dt^2} + \mu_p \frac{d\psi_p}{dt} - J_{go} n_g \frac{d\vartheta_g}{dt} = M_s + M_{zc} \tag{31a}$$

$$J_{gk} \frac{d^2 \vartheta_g}{dt^2} + \mu_g \frac{d\vartheta_g}{dt} + J_{go} n_g \frac{d\psi_p}{dt} = M_{zb} \tag{31b}$$

It should be noted that the frequency of:

$$\Omega_g = \frac{J_{go} n_g}{\sqrt{J_{gk} J_p}} \tag{32}$$

undamped nutation vibrations of GEO is much lower than the frequency of nutation vibrations of the gyroscope of three degrees of freedom, but the respective amplitudes are much higher. Therefore it is always necessary to account for nutation vibrations of the gyroscope executive organ. That results from the fact that, contrary to gyroscope of three degrees of freedom, in the stabilizer $J_p >> J_{gk}$.

In such cases, when the platform (or the aerial object) should be turned by a desired angle value, it is enough to apply moment M_s, worked out by the appropriate program-run device.

For the simplest control law, formed by the amplifier, we can assume:

$$M_s = k_g \vartheta_g \tag{33}$$

Quantity k_g, which occurs in dependence, Eq. (33), is a constant coefficient, whose value depends on static characteristics of elements of stabilization contour: precession angle sensor, amplifier and stabilizing engine.

Though the problem of stability is not considered for gyroscope of three degrees of freedom because it is the very nature of it to maintain stability, the issue becomes of primary importance for stabilizer. Another important problem is to select stabilizer parameters in such a manner so that the transition processes originating in interference moments M_{zb} and M_{zc} would vanish in the shortest possible time, which ensures sufficient stabilization accuracy.

Taking into account that $J_p >> J_{gk}$ and assuming that the OADGS input is caused by non-zero initial conditions and also considering dependence, Eq. (33), in Eq. (31a), the mathematical model of the stabilizer can be written as follows:

$$\frac{d^2\vartheta_g}{dt^2} = -\frac{\mu_g}{J_{gk}}\frac{d\vartheta_g}{dt} - \frac{J_{go}n_g}{J_{gk}}\frac{d\psi_p}{dt} \tag{34a}$$

$$\frac{d^2\psi_p}{dt^2} = \frac{k_g}{J_p}\vartheta_g + \frac{J_{go}n_g}{J_p}\frac{d\vartheta_g}{dt} \tag{34b}$$

By introducing a state vector into the above system:

$$\boldsymbol{x}_g = \begin{bmatrix} \vartheta_g & \dot{\vartheta}_g & \dot{\psi}_g \end{bmatrix} \tag{35}$$

we will obtain the state matrix of the following form:

$$\boldsymbol{A}_g^* = \begin{bmatrix} 0 & 0 & 1 \\ 0 & -\dfrac{\mu_g}{J_{gk}} & -\dfrac{J_{go}n_g}{J_{gk}} \\ \dfrac{k_g}{J_p} & \dfrac{J_{go}n_g}{J_p} & 0 \end{bmatrix} \tag{36}$$

From stability and optimality conditions we will get:

$$k_g > 0, \ \mu_g > 0 \tag{37}$$

$$\mu_g \frac{J_{go}n_g}{J_{gk}} - k_g > 0 \tag{38}$$

$$-\frac{1}{3}\left(\frac{\mu_g}{J_{gk}}\right)^2 - \frac{J_{go}^2 n_g^2}{J_{gk}J_p} > 0 \Rightarrow \mu_g < \sqrt{3}\frac{J_{gk}J_{go}}{\sqrt{J_{gk}J_p}}n_g \tag{39}$$

$$-\frac{2}{27}\left(\frac{\mu_g}{J_{gk}}\right)^3 + \frac{1}{3}\frac{\mu_g}{J_{gk}}\frac{J_{go}^2 n_g^2}{J_{gk}J_p} - \frac{J_{go}n_g}{J_{gk}J_p}k_g = 0 \tag{40}$$

Moreover, from inequality Eq. (39) and condition:

$$\left|Tr\,\boldsymbol{A}_g\right| = \left|-\frac{1}{3}\frac{\mu_g}{J_{gk}}\right| \to max \tag{41}$$

it will ensue that:

$$\mu_g \to \sqrt{3}\frac{J_{gk}J_{go}}{\sqrt{J_{gk}J_p}}n_g \tag{42}$$

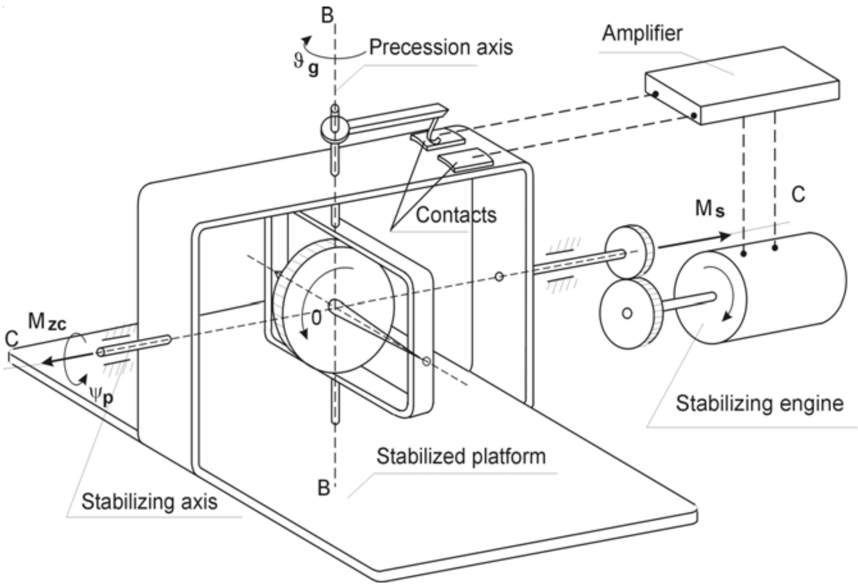

Fig. 7 Principle of operation of one-axial direct gyroscope stabilizer

Thus assuming the maximum value μ_g expressed by Eq. (42) and inserting it into Eq. (40), we will obtain:

$$k_g = \frac{\sqrt{3}}{9} \frac{\sqrt{J_{gk} J_p}}{J_{gk} J_p} J_{go}^2 n_g^2 \tag{43}$$

In this way we have determined unambiguous values of amplification and damping coefficients, for which OADGS will return to the pre-set position in the shortest time.

Taking into account Eq. (38), it is possible to determine the minimum angular velocity of the gyroscope self-rotation from Eq. (43), at which OADGS will be still stable:

$$n_{g\,min} = \sqrt[4]{3 J_{gk} J_p}\, \frac{\sqrt{3k_g}}{3J_{go}} \tag{44}$$

Determining the optimum velocity of self-rotation from Eq. (43):

$$n_{g\,opt} = \sqrt[4]{3 J_{gk} J_p}\, \frac{\sqrt{3k_g}}{J_{go}} \tag{45}$$

we will note that those velocities hold the following relations:

$$n_{g\,opt} = 3\, n_{g\,min} \tag{46}$$

In Figures 8 and 9, the areas of permissible changes and the optimum angular velocities of self-rotation depending on changes in OADGS parameters are presented in a graphic form. The following notation is introduced in figure:

$$\hat{J}_g = \frac{\sqrt[4]{J_{gk} J_p}}{J_{go}} \tag{47}$$

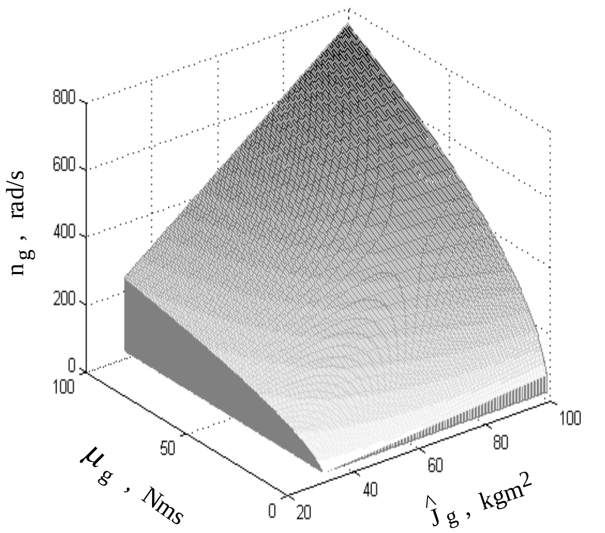

Fig. 8 Dependence of the minimum stable angular velocity n_g of OADGS on dumping coefficient μ_g and quantity $\hat{J}_g$

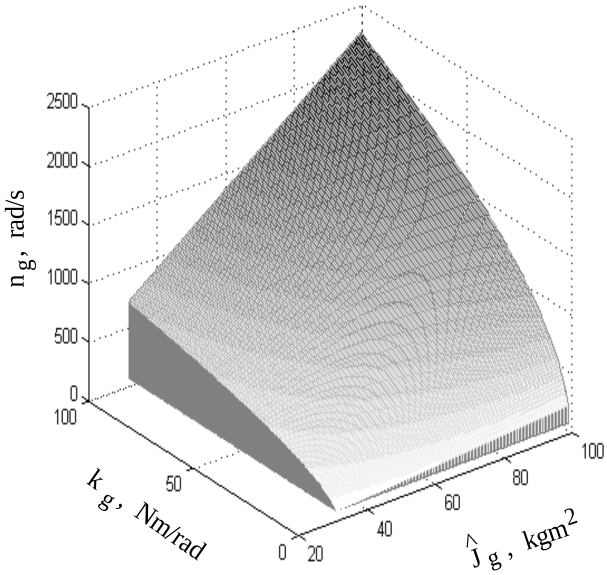

Fig. 9 Dependence of the optimum stable angular velocity n_g of OADGS on amplification coefficient k_g and quantity $\hat{J}_g$

6. OPTIMUM CORRECTION FOR TWO-AXIAL DIRECT GYROSCOPE STABILIZER (TADGS)

In two-axial stabilizer (Figure 10), gyroscope can rotate around axes of both frames. Signals corresponding to those rotations are transferred to two stabilizing engines through an amplifier. The engines have to eliminate interference deflections, because of which the gyroscope starts turning in the opposite direction. Let us assume that correction moments are proportional to rotation angles. Then, if an ideal operation of the stabilization system is assumed, we can write:

$$M_b^k = -k_b \vartheta_g,\; M_c^k = k_c \psi_p \tag{48}$$

Taking into account the proportionality of velocities of damping moments in respect of both axes, the stabilizer motion equation for small deflection angles reads as follows:

$$\frac{d^2\vartheta_g}{dt^2} = -\frac{h_b}{J_{gk}}\frac{d\vartheta_g}{dt} - \frac{J_{go} n_g}{J_{gk}}\frac{d\psi_p}{dt} - \frac{k_b}{J_{gk}}\vartheta_g + M_{zb} \tag{49a}$$

$$\frac{d^2\psi_p}{dt^2} = -\frac{h_c}{J_p}\frac{d\psi_p}{dt} + \frac{J_{go} n_g}{J_p}\frac{d\vartheta_g}{dt} + \frac{k_c}{J_p}\psi_p + M_{zc} \tag{49b}$$

where h_b, h_c are coefficients of damping moments.

Let the system described by Eq. (49) be presented in vector-matrix form:

$$\dot{\boldsymbol{x}}_g = \boldsymbol{A}_g \boldsymbol{x}_g \tag{50}$$

where:

$$\boldsymbol{x}_g = \begin{bmatrix} \vartheta_g & \frac{d\vartheta_g}{d\tau} & \psi_p & \frac{d\psi_p}{d\tau} \end{bmatrix}$$

$$\tau = \Omega t; \quad \Omega = \frac{J_{go} n_g}{\sqrt{J_p J_{gk}}};$$

$$\boldsymbol{A}_g = \begin{bmatrix} 0 & 1 & 0 & 0 \\ -\bar{k}_b & -\bar{h}_b & 0 & -\sqrt{\frac{J_p}{J_{gk}}} \\ 0 & 0 & 0 & 1 \\ 0 & \sqrt{\frac{J_{gk}}{J_p}} & \bar{k}_b & -\bar{h}_c \end{bmatrix};$$

$$\bar{k}_b = \frac{k_b}{J_{gk}\Omega^2}; \quad \bar{k}_c = \frac{k_c}{J_{gk}\Omega^2}.$$

Applying, as in the previous case, the modified Golubiencew optimization method, we will determine such coefficients k_b, k_c, h_b, h_c, for which the transition process in TADGS will disappear in the shortest time. Analytical dependences obtained will not be quoted because of the limited scope of the present paper.

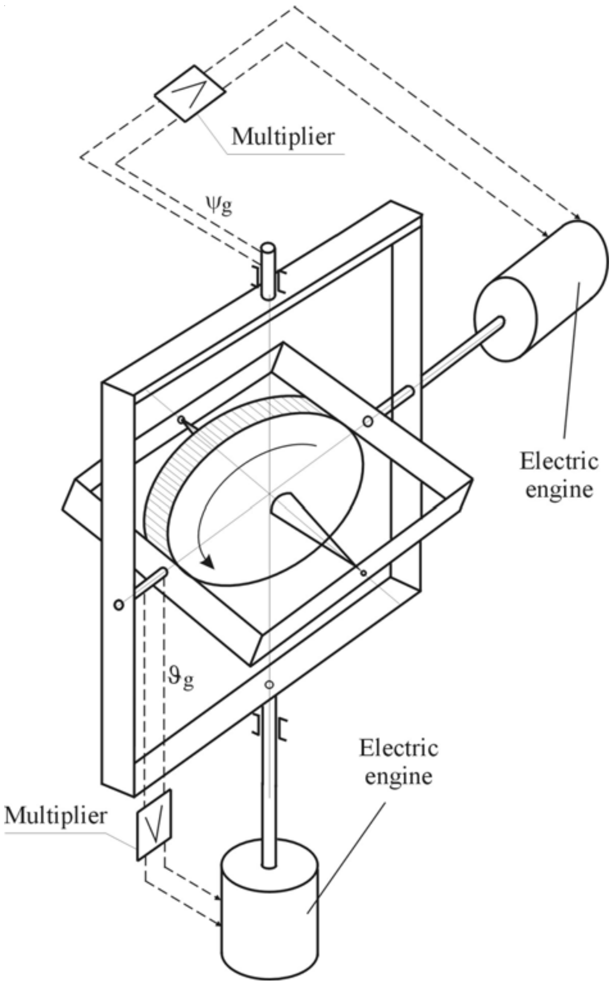

Fig. 10 General view of two-axial direct gyroscope stabilizer

7. CONCLUSIONS

Gyroscope as the executive organ of control in the guidance systems of aerial objects (homing rocket missiles, guided bombs, etc.) has two basic advantages: a) the moment from the engine is transmitted directly, without complex systems of levers and gears; b) the transmission of the control moment takes place with amplification effect - the engine transmits much lower moment than it is the case with other executive organs.

Moreover, the basic advantage of a light aerial object homing with a direct gyroscope stabilizer is its great autonomy and the fact that a complex optical system can be entirely eliminated.

As gyroscope is strongly a non-linear system, at high values of gyroscope axis deflections and angular velocities, there appear errors in the pre-set motion in relation to that actually performed. Thus gyroscope programme-run control in its non-linear operation range and under the interference conditions must be accompanied by additional optimum control in a closed system.

The algorithm for the selection of the controlled gyroscope system optimum parameters put forward in the present paper provides for the minimization of discrepancies between pre-set path and the one actually exercised. We have the option to change, in real time, the regulator coefficients depending on change in self-rotation angular velocity as the function of time. If we deal with a gyroscope and regulator of already set parameters, it is possible to select the optimum angular velocity of self-rotation as the function of these parameters.

8. REFERENCES

[1] Z. Koruba, *Dynamics and Control of Gyroscope on the Board of Aerial Vehicle*, Monographs, Studies, Dissertations, No. 25, Kielce University of Technology, Kielce, 2001. (in Polish)

[2] K. Magnus, *Kreisel - Theorie und Anwendungen*, Springer-Verlag, Berlin-Heidelberg-New York, 1971. (translated into Russian: K. Magnus, Giroskop: Teorija i primenenije, Mir, Moskva, 1974.)

[3] M.A. Pavlovski, *Theory of Gyroscope*, Viša škola, Kiev, 1986. (in Russian)

[4] Z. Koruba, Selection of the optimum parameters of the gyroscope system on elastic suspension in the homing missile system, *Journal of Technical Phisycs*, Vol. 40, No. 3, Polish Academy of Sciences, Institute of Fundamental Technological Research, Warszawa Military University of Technology, Warszawa, pp. 341-354, 1999.

[5] Z. Koruba, Gyroscope dynamics and control in homing rocket with autonomous system of target location, *Journal of Technical Phisycs*, Vol. 41, No. 3, Polish Academy of Sciences, Institute of Fundamental Technological Research, Warszawa Military University of Technology, Warszawa, pp. 253-273, 2000.

[6] Z. Koruba and J. Osiecki, *Construction, Dynamics and Navigation of Close-Range Missiles - part I*, University course book, No. 348, Kielce University of Technology Publishing House, Kielce, 1999. (in Polish)

[7] S. Dubiel, Generalized constraints and their application in studying controllability of flying objects, Supplement Bulletin of Military University of Technology, Warszawa, 1973. (in Polish)

[8] Z. Koruba, Adaptive correction of controlled gyroscope on the deck of aerial object, *Journal of Technical Phisycs*, Vol. 42, No. 2, Polish Academy of Sciences, Institute of Fundamental Technological Research, Warsaw Military University of Technology, Warszawa, pp. 203-222, 2001.

ALGORITAM KONTROLE I KOREKCIJE DIREKTNOG GIROSKOPSKOG STABILIZATORA

SAŽETAK

Ovaj rad prikazuje analizu stabilizacije i točnosti giroskopskog stabilizatora koji se koristi za automatsku kontrolu i navođenje letećih objekata. Postojanje međusobnih veza između kanala multiaksijalnog giroskopskog stabilizatora uzrokuje greške u radu ovog uređaja. Stoga je potrebno odabrati optimalne parametre za sve elemente stabilizacijskih kanala. U ovome radu daje se algoritam optimalne selekcije gore spomenutih parametara kao i rezultati ispitivanja kompjutorske simulacije.

Ključne riječi: *Giroskopski stabilizator, navođenje letećih objekata, automatska kontrola, stabilizacijski element, Golubienceva metoda optimizacije.*